

Structural monitoring of a wind turbine steel tower – Part II: monitoring results

C. Rebelo^{*1}, M. Veljkovic², R. Matos¹ and L. Simões da Silva¹

¹*ISISE, Civil Engineering Department, University of Coimbra, Rua Luís Reis Santos, Coimbra, Portugal*

²*Luleå University of Technology, SE-97187 Luleå, Sweden*

(Received March 8, 2011, Revised August 30, 2011, Accepted August 31, 2011)

Abstract. This paper presents results from the structural monitoring of a steel wind tower characterized and presented in Part I of the paper. Monitoring period corresponds to about fifteen months of measurements. Results presented refer to stress distribution on shell and in bolts at different heights, stress fatigue spectra, section forces along height evaluated from the stress measurements and comparison with design forces, dynamic response in terms of accelerations, stresses, deflections and rotations.

Keywords: Wind tower; steel; monitoring; wind loading; fatigue; dynamic response

1. Introduction

This paper presents monitoring results obtained after calibration and tests on the monitoring system of the steel wind tower described in Part I of this paper (Rebelo 2011). The total monitoring period is about fifteen months, between September 2009 and November 2010. In the first phase (Phase I) of the monitoring period, until the end of April 2010, the signal recording was activated either manually or automatically for wind speeds over 4 m/s and a total of 390 records were registered. During the second phase (Phase II) corresponding to the period from April to November 2010 the trigger level was updated to wind velocities greater than 14 m/s and a total of 660 records were registered. When automatically started by the trigger the recording is activated during one hour independently of the wind speed and after that period the trigger becomes active again. Therefore, during persistent strong wind the recording is almost continuous.

Throughout the monitoring period there were interruptions due to system malfunction or maintenance works in the tower to make some adjustments in the data transmission system. Some of the interruptions were relatively long, taking some days or even weeks. During Phase I system was active during 58% of time (139 days out of 240) and during Phase II system was active during 75% of time (159 days out of 210). For safety reasons, during all the time, the access to the interior of the tower was only possible if accompanied by members of the maintenance staff contracted by the owner of the tower. The possibility of having some equipment (e.g., computer, *GSM* module, etc.) outside the tower, and therefore accessible without restrictions, was not considered because of security reasons (vandalism, robbery). Nevertheless, the main reason of the system inactivity, after

* Corresponding author, Assistant professor, E-mail: crebelo@dec.uc.pt

preliminary tests, was simply lack of electric power inside the tower. The circuit breakers of the electric circuit used by the equipment were breaking frequently and it could take several days even weeks to get authorization for accessing the tower for reparation. The replacement of the circuit breaker with a more powerful one had to be accepted by the maintenance team, who try to avoid changes in the original circuits because of liability reasons.

In order to numerically simulate the measurements results that are obtained from the monitoring a finite element model of the tower was developed whose updating by modal identification was included in Part I of the paper (Rebelo 2011). It allows for the comparison between measured and computed response and gives the output of the results matching the type and the location of the sensors used for monitoring. The developed FE model is in accordance with the available production drawings of the eighty meters high steel tower supporting a 2.1 MW turbine Wind Class III IEC2a erected in the central part of Portugal. The software *LUSAS* (Lusas, v14a,b) was used for the modelling and the response calculation. The structural computations presented are based on linear elastic analysis and include soil-foundation interaction (Adhikari and Bhattacharya 2011, Bowles 1988).

2. Strain measurements

2.1 Shell

The monitoring system acquires strain signals using two different sampling rates, low frequency at 2.5 Hz and high frequency at 100 Hz. In order to analyse the evolution of the signals during the whole monitoring period the second type of signals were decimated and sampled at 2.5 Hz. The entire time series (Phase II) of two strain gauges at level 0, wind speed and nacelle orientation are given in Fig. 1. The sensors' locations are given in Table 1. The time series corresponds to the

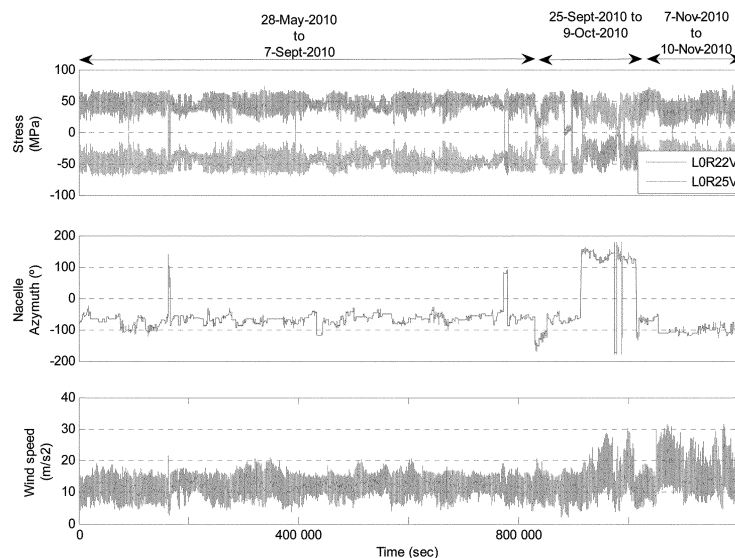
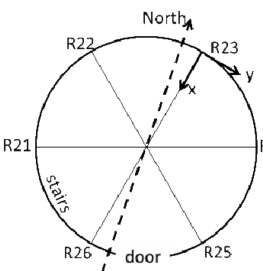
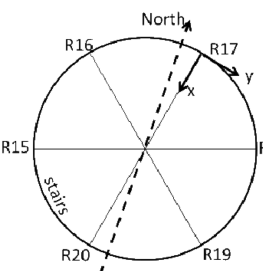
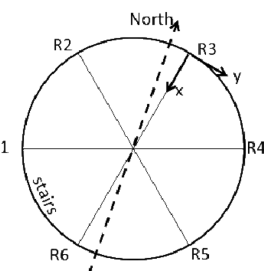
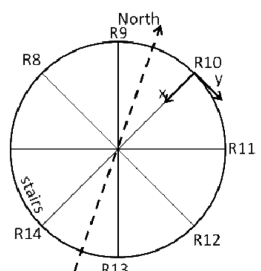


Fig. 1 Time signals obtained during Phase II with trigger based on wind speed greater than 14m/s (a) vertical stress at strain sensors L0R22V and L0R25V, (b) nacelle azimuth – positive direction is clockwise and (c) wind speed

Table 1 Sensors' locations

Level 0	Level 1	Level 2	Level 3
			
Initials for Signals' identification: L(1)(2)(3)(4)	(1) Level number (2) Type of signal: R – strain gauge Rosette Acc – accelerometer B – strain gauge in bolt Inc – inclinometer	(3) Strain gauge direction in rosettes V – vertical tower axis H – horizontal along section perimeter D – diagonal	e.g., L2R21D : Level 2, Rosette 21, strain gauge in Diagonal direction

sequence of measurements made during the monitoring period put together in a continuous time line. Therefore, most of the abrupt changes in the signal are due to the fact that between the end of a segment and the beginning of the next segment there is in reality a time gap depending on the measurement conditions and interruptions.

Considering the dominant direction of the nacelle the measurement points at L0R22V and L0R25V are at the most stressed part of the tower section by bending. The trigger is set to a wind speed of 14 m/s resulting in a relatively high mean wind speed of about 12.8 m/s, which corresponds to the maximum loading imposed during normal operation of the turbine.

In order to visualize the evolution of the shell stresses depending on wind speed, the maximum tensile and compressive stresses were computed from the measured time series segmented in periods of 10 seconds. These extreme values are plotted in Fig. 2 against the corresponding 10-seconds mean wind speed. Maximum stresses are achieved between 10 and 14 m/s wind speed decreasing to a steady state level for higher wind velocities. This effect is due to the regulation of pitch angle for higher wind speeds, that is, the blade angle varies in order to decrease the tower loading while maintaining the production rates (Burton *et al.* 2001, Hau 2006, Veljkovic *et al.* 2011).

For the sake of comparison, stress computations were performed using the calibrated model

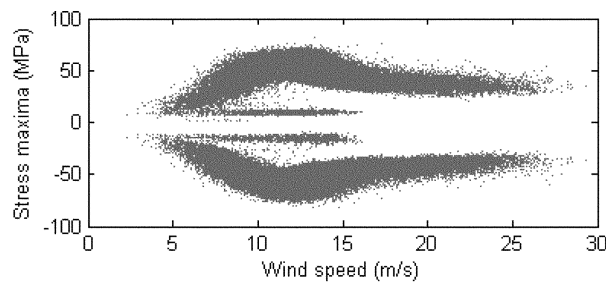


Fig. 2 Extreme vertical stresses in the shell at levels 0 and 1 plotted against 10-seconds mean wind speed

Table 2 Vertical stresses computed from design load cases given for the instrumented tower

Section	Bending moment (kN.m)		Bending stress (MPa)	
	<i>DLC 1.3</i>	<i>DLC 1.5</i>	<i>DLC 1.3</i>	<i>DLC 1.5</i>
Bottom	14799.0	48196.4	34.0	110.6
Level 0	13947.1	44925.6	38.6	124.2
Level 1	12051.3	37378.4	43.8	135.7
Level 2	8531.1	21048.1	51.4	126.9
Level 3	5752.1	4961.7	65.6	56.6
Top	5227.9	1665.4	42.4	13.5

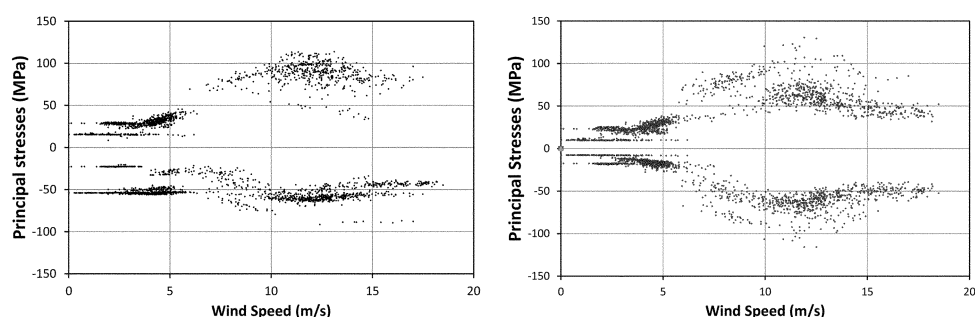


Fig. 3 Principal stresses in the shell at levels 0 and 1 plotted against 10-seconds mean wind speed

(Rebelo 2011) and the load resultants given by the tower producer for several tower elevations. Two design load cases were considered of the type dlc 1.3 and dlc 1.5 (Germanischer Lloyd 2003), which correspond to the simulation of the one-year-gust in combination with the loss of electrical connection followed by the rotor start positions which lead to the most unfavourable conditions for the wind tower. The stresses are given in Table 2 and are computed from the section loads without safety factor given in the design load tables of the tower manufacturer. The wind speed is 26 m/s and 9 m/s respectively and the wind direction relative to the nacelle orientation is 65.5° and 0.1° respectively for dlc 1.3 and dlc 1.5. The maximum measured stresses at levels 0 and 1 given in Fig. 2 are bounded by the design values of Table 2.

At each measurement point three stress directions are measured. Therefore, the principal stresses can be computed and are presented in Fig. 3 for levels 0 and 1. The highest principal stresses occur for wind speeds of about 12 m/s with maximum values of about 130 MPa.

2.2 Bolts

Due to the pre-stress in the bolts, the stresses measured during operation are expected to be much smaller than those in the shell. Fig. 4 shows the difference between the stress variation in the bolts and the corresponding vertical stress in the shell. It is noted that the mean stress in the bolts is always negative revealing that between the time of calibration and the time of measurement there was loss of pre-stress in the bolts. Some of the bolts (e.g., L1B6) present an unsteady behaviour which is justified on one side by the natural interruption of the time line associated with the sequence of different recorded segments and on the other side by the adjustments of pre-stress in

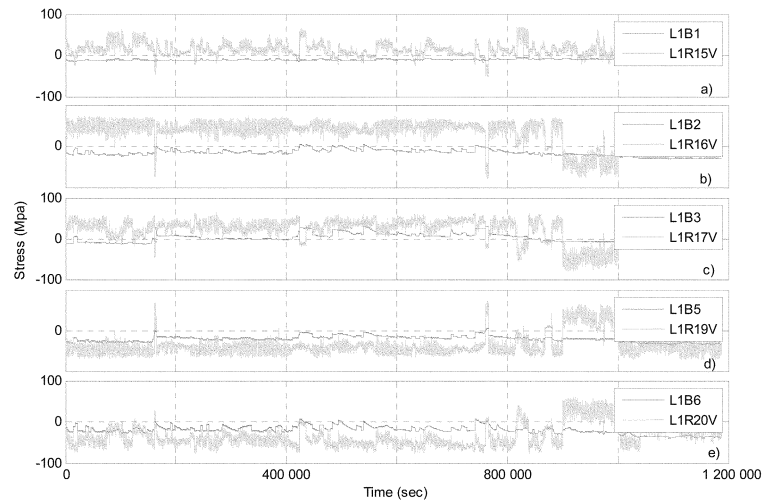


Fig. 4 Comparison of stresses in bolts (dark curves) with vertical stresses in shell at level 1 during the second measurement period: (a) L1B1 – L1R15V, (b) L1B2 – L1R16V, (c) L1B3 – L1R17V, (d) L1B5 – L1R19V and (e) L1B6 – L1R20V

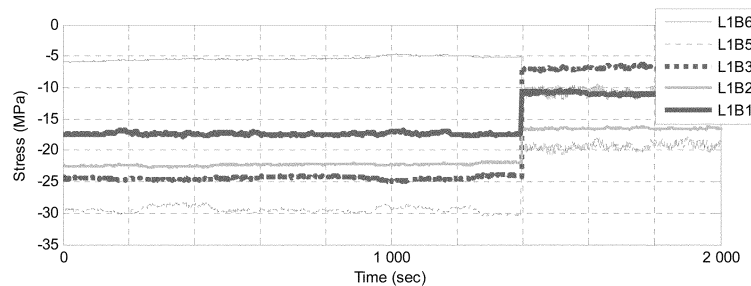


Fig. 5 Stress increase in the bolts due to retightening

the measured bolt influenced by the alterations of the pre-stress in the neighbouring bolts (Veljkovic 2010a,b). One must be aware that, in this connection there are 6 instrumented bolts among a total of 124 bolts. However, when all the instrumented bolts present an increase of tension, this can be correlated with the maintenance work performed in the tower that includes retightening of the bolts. This is illustrated in Fig. 5 where all bolts suffered a synchronized increase in stress, except the first which decreased the stress.

2.3 Fatigue spectra

Fatigue spectra were calculated for the shell vertical stresses using the rainflow method. The original spectra were computed from measured time series with totals of 0.68×10^6 and 1.2×10^6 seconds length corresponding to monitoring periods of 139 and 159 days, respectively, for Phase I and Phase II. Subsequently, the number of cycles was linearly extrapolated for a 20 years lifetime (20×365 days) and the obtained spectra are given in Fig. 6. Differences in curves obtained for different phases are mainly due to the difference in the mean wind loading associated to the monitoring phases, that is, for Phase I with a lower mean wind speed the number of cycles

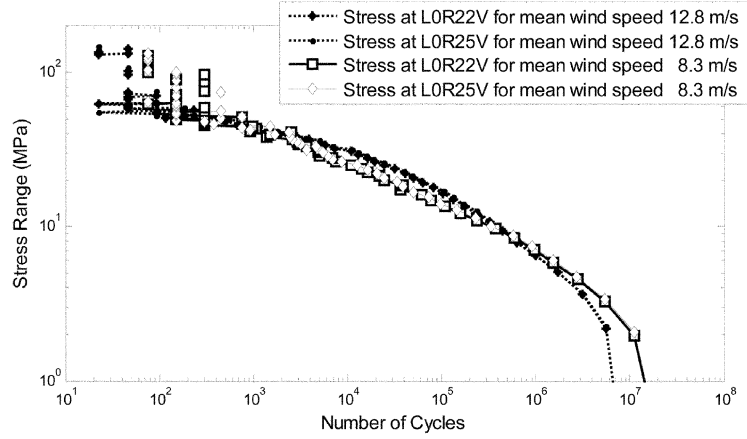


Fig. 6 Measured fatigue spectra extrapolated for 20 years lifetime obtained for level 0

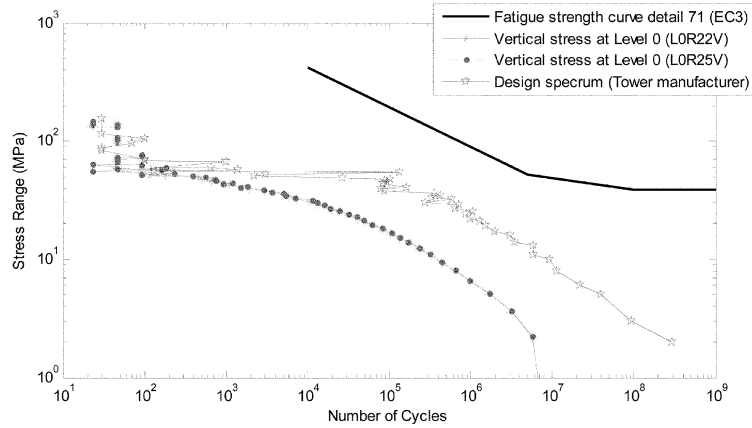


Fig. 7 Comparison of measured fatigue spectrum extrapolated for 20 years lifetime with design spectrum and strength curve obtained from EN1993-9 for detail 71

increases in lower stress ranges and decreases in the upper stress ranges.

The comparison between the measured spectra and the design load spectra given by the tower designer, as well as with the fatigue strength curve given by EN1993-1-9 (CEN 2005) for fatigue detail 71, are shown in Fig. 7. According to the Palmgren-Miner rule used in Annex A of the eurocode (CEN 2005) with $\gamma_{Mf} = 1.35$ and $\gamma_{Ff} = 1.0$ the damage index obtained for the stress history at point L0R22V during the Phase II is $D = 7.4 \times 10^{-4}$. To compute the lifetime the most unfavorable situation would be based on the length of the measured time series, which gives

$$\text{Lifetime} = \frac{\text{Time(year)}}{D} = \frac{12 \times 10^6}{3600 \times 24 \times 365 \times 7.4 \times 10^{-4}} = 51 \text{ years} \quad (1)$$

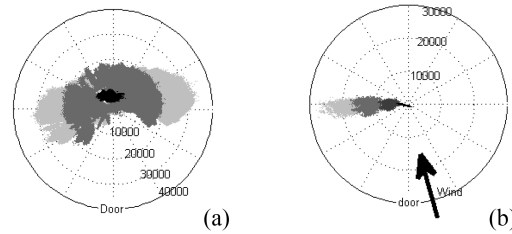


Fig. 8 Bending moment vectors represented by their amplitude and direction in polar coordinates, (a) entire Phase II and (b) selected 2000 seconds

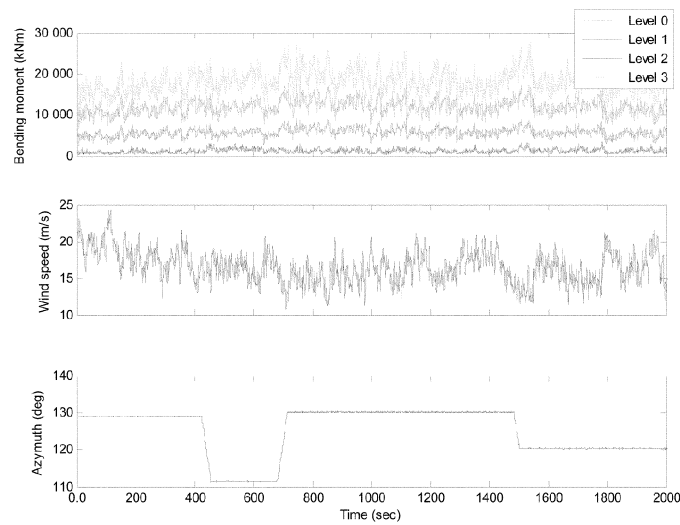


Fig. 9 Typical time histories for bending moments obtained from strain measurements during wind speed average of 16.5 m/s

3. Section load resultants

The signals obtained directly from the measuring instruments can be converted in section resultants and in displacements using the known geometry of the tower. Fig. 8(a) represents the bending moment vectors obtained from the shell stresses at different levels for each time increment of the measurements in Phase II. The representation of each vector is only one point in the polar coordinates of the diagram. Bending moments at lower level are represented with lighter grey marks and at upper levels in darker grey marks. The bending moment vectors' dominant direction is orthogonal to the dominant wind direction as expected. Fig. 8(b) shows the same representation for a shorter period of about thirty minutes, which is the same time window used to represent time histories in Fig. 9. These are typical time histories of the bending moments at different levels obtained during wind speed average of 16.5 m/s and nacelle azimuth average of 120° . A representation of the bending diagrams of M_x , M_y and resultant M along tower height for the same time period is shown in Fig. 10. Comparing with design bending moments given in Table 2, measured values are in the range of values given for DLC13.

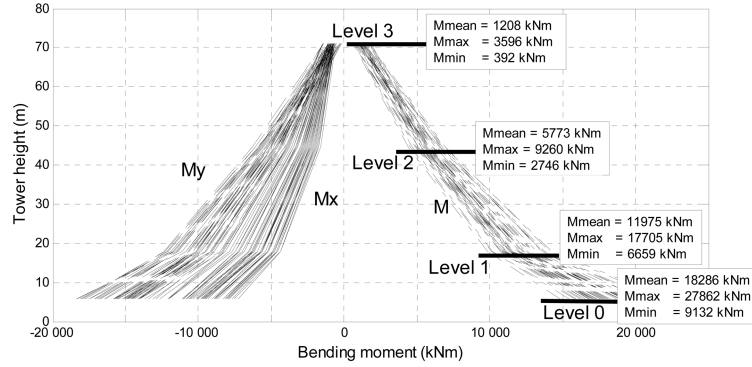


Fig. 10 Bending moments M_x , M_y and resultant M obtained from selected shell stress measurements; mean values over 40 seconds; wind speed average is 16.5 m/s

4. Dynamic response

4.1. Accelerations

The blades of the horizontal-axis wind turbine rotate in close proximity to the tower and important dynamic loading is induced when passing in front of the tower. The blade-passing frequency is equal to the turbine rotational frequency multiplied by the number of blades on the turbine rotor, which is three. The dynamic response of the wind tower is mainly due to the turbine rotation and is therefore almost periodic.

To avoid large vibration amplitudes the lowest natural frequencies of the tower should be kept away from the rotational and/or blade-passing frequencies and their harmonics. Analysing the spectra obtained from the measurements of the accelerations at the top of the tower (see Fig. 11) three peaks are clearly identified in the range 0 Hz to 1 Hz and several other peaks are identified up

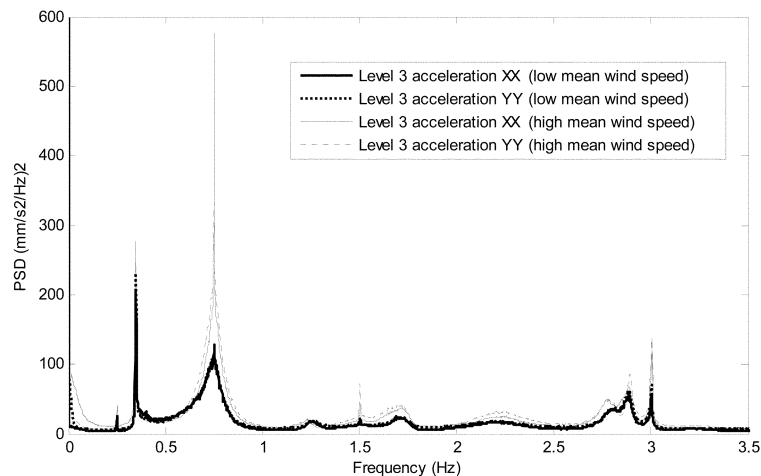


Fig. 11 Power spectral densities of the acceleration at the tower level 3 obtained during operation

to 3 Hz. The first peak in the spectrum corresponds to the rotational frequency of 0.25 Hz. The wind turbine manufacturer gives operating limits of 0.13 Hz and 0.25 Hz, for the lower and upper rotor speed, respectively. The upper limit is attained for average wind speeds around 12 m/s, which is in the range of wind speed for which recording of the monitored signals is activated. The second spectral peak is at frequency 0.34 Hz and corresponds to the first and second natural frequencies of the tower. The damping ratio measured during operation in these modes is 1.12%, close to the value obtained in the modal identification (Rebelo, *wo/d*). The third peak in the spectrum corresponds to the blade passing frequency of 0.75 Hz.

It is expected that the wind load acting on the tower increases up to a certain limit defined by the type of turbine, in this case the load increases up to average wind speeds of about 12 m/s. This effect can be observed in the spectral values shown in Fig. 11 which increase for the time series corresponding to higher wind speed average (Phase II). The peaks at 1.5 Hz and 3.0 Hz are harmonics of the blade passing frequency. The third and fourth natural frequencies appear at about 2.8 Hz near the third harmonic of the blade passing frequency. The measured damping was 1.4% and therefore higher than the one measured during modal identification.

4.2 Displacements

The design guidelines do not establish general limits for displacement of the tower. However, rules are given (IEC 2005, DNV/Risø 2002, GL 2003) to compute the displacements and to verify that deflections do not affect structural integrity in the design conditions, e.g., no mechanical interference between blade and tower will occur. These deflections are composed by tower and blade displacements. Concerning the tower, the deflections are minimized by avoiding resonance and, therefore, by limiting the dynamic displacements. Note that the clearance between blade and tower is not only governed by the structural deflections, but also by a possible slip at the yaw bearing, by the perpendicularity of the tower flange, and by the tolerances on the tilt and on the rotor plane. (DNV/Risø 2002, GL 2003)

The rotations at levels 2 and 3 are obtained directly from the inclinometers. Fig. 12 shows a typical measured time history of tower inclination. The mean value of the measured rotation in the time window is 0.20° for Level 3 and 0.18° for Level 2.

Displacements can be obtained from integration of the accelerations, although only the dynamic part of the signal can be obtained (see Fig. 13). Integration error was controlled through Baseline Correction and Filtering (Bendat and Piersol 1993, Dally *et al.* 1993). The first process consists on (i) determining, through regression analysis (least-squares-fit method), the straight line that best fits

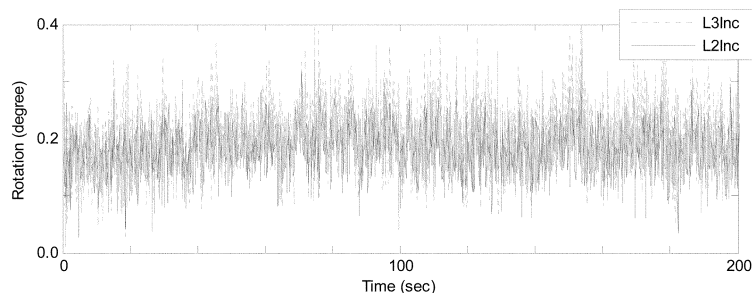


Fig. 12 Typical time window of tower inclination measured at levels 2 and 3

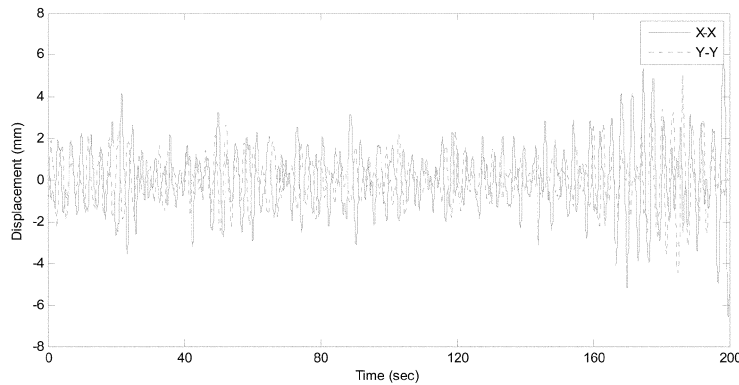


Fig. 13 Typical time window of horizontal displacements at level 3 in x - and y -direction obtained from time integration of filtered accelerations using a highpass Butterworth filter above 0.2 Hz

the time-acceleration pairs of values and then (ii) subtracting from the actual acceleration values their corresponding counterparts as obtained with the regression-derived equation. In this manner, spurious baseline trends, usually well noticeable in the displacement time-history obtained from double time-integration of uncorrected acceleration history, are removed. Afterwards a Butterworth high pass filter above 0.2 Hz was applied in order to remove low frequency components not removed by the former procedure. Data processing was performed using Matlab (The MathWorks 2010).

5. Conclusions

The monitoring system developed for the steel tower is working as foreseen. This paper presents some measurement results which have been obtained during about fifteen months.

First, there was the need to assure the quality of the measured data. It was verified that, at each cross section, the sum of the vertical stresses was, as expected, near zero, since only stresses due to bending are measured. As expected, stress variations along the tower height are low, since the cross section varies in diameter and thickness along the height, corresponding to a optimized the structural solution.

The strains measured on the cylinder shell (vertical, horizontal and inclined) vary with wind speed, increasing up to a wind speed of about 12 m/s and decreasing beyond that. This is typical of pitch regulated towers and is due to the pitch rotation of blades in order to maintain a constant production without overloading the tower. The maximum measured principal stress in the shell was about 130 MPa, and the maximum vertical stress was about 70 MPa.

The stress variation inside the pre-stressed bolts is low and therefore almost independent of the wind speed. It is concluded that the bolt pre-stress is very effective and there is a good contact between the flanges. This is an expected conclusion because it is not probable that service loads, mainly from measured wind speeds up to 20 m/s, could induce the opening of the joints between the stiffening rings of the connection.

Stress fatigue spectra can be computed for the measured data. The spectra obtained for the shell stresses at level 0 section were extrapolated to twenty years lifetime. They are clearly below the design spectra as expected, except for the higher stress ranges. Longer data acquisition will allow more clarification of this issue, since the number of large stress ranges is relatively low.

Dynamic response is evaluated through the acceleration spectra. It is clear that no resonance occurs in the tower in the range of identified natural frequencies. The dynamic deflections are computed by integration of the accelerations and therefore represent only the dynamic part of the response.

The monitoring system remains active and it is expected that continuous measurements of strains will allow better estimates of the real stress fatigue spectrum of the shell. Also, measurement of accelerations will allow detection of eventual changes in the response vibration spectrum and therefore, structural health monitoring of the tower including foundation. Also the monitoring of the stress inside the bolts may infer about the real pre-stress losses experienced during the service life.

Acknowledgements

The authors are grateful for the financial support of the RFCS (Research Fund for Coal and Steel of the European Community) under the contract RFSR-CT-2006-00031. The collaboration of all project partners is warmly thanked. Furthermore, the authors thank Eng. José Saraiva (Repower Portugal) for the support during maintenance works.

References

- Adhikari, S. and Bhattacharya, S. (2011), “Vibrations of wind-turbines considering soil-structure interaction”, *Wind Struct.*, 14(2), 85-112.
- Bendat, J.S. and Piersol, A.G. (1993), *Engineering application of correlation and spectral analysis*, John Wiley & Sons.
- Bowles, J.E. (1988), *Foundation analysis and design*, McGraw-Hill.
- Burton, T., Sharpe, D., Jenkins, N. and Bossanyi, E. (2001), *Wind energy handbook*, John Wiley & Sons.
- CEN, (2005), *EN 1993-1-9: Design of steel structures - Part 1-9: Fatigue*, Brussels.
- DNV/Risø, (2002), *Guidelines for design of wind turbines*, 2nd Ed., Copenhagen.
- Dally, J.W., Riley, W.F. and McConnell, K.G. (1993), *Instrumentation for engineering measurements*, 2nd Ed., John Wiley & Sons.
- GL-Deutsche Gesellschaft für Luft- und Raumfahrt (2003), *Guideline for the certification of wind turbines*.
- Hau, E. (2006), *Wind Turbines: fundamentals, technologies, application, economics*, Springer, Berlin.
- IEC (2005), International Standard 61400-1, 3rd Ed., Wind turbines – Part 1: Design requirements.
- LUSAS, Element Reference Manual – version 14a, UK.
- LUSAS, Modeller Reference Manual – version 14b, UK.
- The MathWorks Inc., MATLAB version 2010, Natick, MA, 2010.
- Rebelo, C., Veljkovic, M., Simões da Silva, L., Simões, R. and Henriques, J. (2011) “Structural monitoring of a wind turbine steel tower – Part I: system description and calibration”, *Wind Struct.*
- Veljkovic, M. et al. (2012a), *High-strength tower in steel for wind turbine*, Final Report, RFSR-CT-2006- 00031. Brussels: RFCS publications, European Commission.
- Veljkovic, M. et al. (2010b), “Friction connection in tubular towers for wind turbines”, *Stahlbau*, 79(9), 660-668. DOI: 10.1002/stab.201001365
- Veljkovic, M. et al. (2011), “Wind turbine tower design, erection and maintenance”, in *Wind energy systems: Optimising design and construction for safe and reliable operation* Edited by J D Sørensen, Aalborg University and J N Sørensen, Technical University of Denmark, Denmark, Woodhead Publishing Limited, Cambridge, UK.